Czech Technical University in Prague
Faculty of Nuclear Sciences and Physical Engineering
Department of Physics

The Influence of the Voltage Uncertainty of the Electron Spectrometer on the Determination of the Conversion Line Energy in the Transition-9.4 keV of ^{83m}Kr

Research work

Author: Bc. Miroslav Krůs
Supervisor: RNDr. Miloš Ryšavý, CSc.
Consultant: prom. fyz. Drahoslav Vénos, CSc.
Academic year: 2006/2007

Abstract

Up to this date, energetically well defined nuclear standards do not exist for the electron spectroscopy. Such a standard, for conversion electrons from transitions in $^{83m}\mathrm{Kr}$, is being developed at Řež and it will be utilized in an independent device for the monitoring of the voltage on main spectrometer of the prepared experiment KATRIN. The quality of the developed source is tested by measurement at the electrostatic spectrometer ESA12 in NPI Řež. The aim of this work is to determine, how the uncertainty of conversion electrons energy depends on the uncertainty of voltage that is applied on electrodes of the spectrometer and uncertainty which is induced in measurement of this voltage by a voltmeter.

KEYWORDS: KATRIN, monitoring, conversion electrons, electron nuclear standard

Abstrakt

V jaderné fyzice dosud neexistují energeticky dobře definované jaderné standardy pro elektronovou spektroskopii. Jeden takový standard - konverzní elektrony z přechodů v $^{83m}\mathrm{Kr}$ - je vyvíjen v Řeži a bude použit v nezávislém kontrolním zařízení pro monitorování napětí na hlavním spektrometru připravovaného experimentu KATRIN. Kvalita vyvíjeného zdroje je testována měřením na elektrostatickém spektrometru ESA12 v ÚJF Řež. Cílem této práce je určit, jak závisí nejistota v určení energie konverzních elektronů na nejistotě napětí, které je přiloženo na elektrody spektrometru, a nejistotě s jakou je toto napětí měřeno voltmetrem.

KLÍČOVÁ SLOVA: KATRIN, monitorování, konverzní elektrony, elektronový jaderný standard

Acknowledgments

I am very grateful to both my supervisors Miloš Ryšavý and Drahoslav Vénos for their help and, above all, for their enormous patience during the preparing of this work. Also I would like to thank them for lending the articles and books which were necessary for my work. Further I would like to thank Otokar Dragoun, Antonín Špalek, and Jaromír Kašpar for their ideas and suggestions that have got the significant influence on this work.

Contents

1 Introduction

One of the most challenging task in modern physics is to determine the rest mass of neutrino. This particle has a fundamental implication to particle physics, astrophysics and cosmology. In particle physics, the Standard Model assumes that neutrinos are massless particles. However, the recent investigations with solar and atmospheric (created by cosmic rays) neutrinos show that neutrinos oscillate when they are travelling along their path (i.e., for example, electron neutrino is transformed into muon or tauon neutrino). The neutrino oscillations are a strong evidence for massive neutrinos.
Neutrinos play very important role in astrophysics and cosmology, too. They carry away up to 99 % of the energy that is released in the supernova explosion. The cosmological implication of zero neutrino mass is such that we know only 4 % of the composition of our Universe (so called visible matter). The remainder mass of the Universe is unknown and massive neutrino can contribute to this invisible part of our Universe considerably.

The aim of prepared experiment KATRIN [1] is a determination of the mass of neutrino from the shape of the end of β-spectrum of tritium (see Figure 1). This experiment will improve the sensitivity on neutrino mass by factor ten in comparison with previous experiments in Mainz [2] and Troitsk [3].

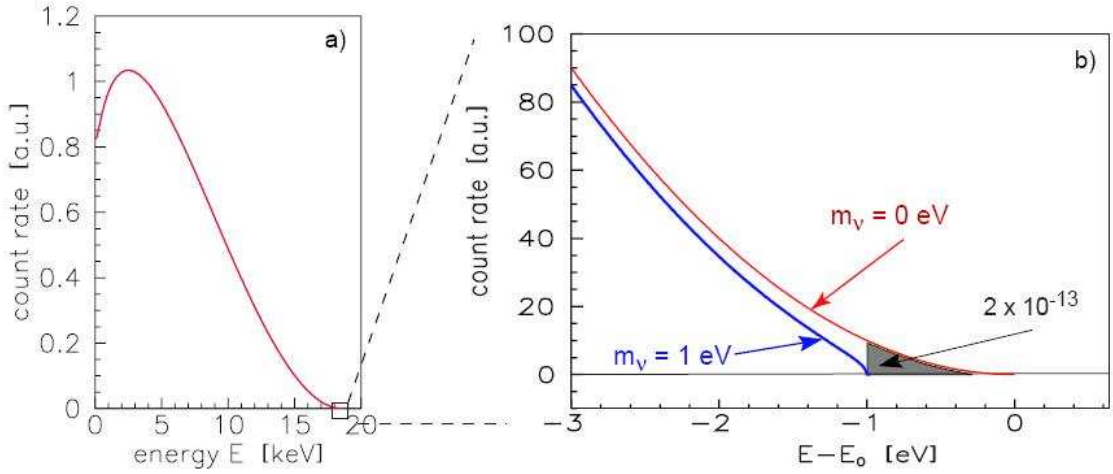

Figure 1: The electron energy spectrum of tritium β decay: (a) complete and (b) narrow region around endpoint energy E_0. In (b), the β spectrum is shown for neutrino mass of 0 or 1 eV.

The tritium was chosen due to its several advantages:

- tritium decays by super-allowed transition with a half life of 12.3 years
- it has the simplest atomic shell
- it has one of the lowest endpoint energy (18.6 keV)

The experimental setup of KATRIN (Figure 2) can be divided into four major units:

- Windowless Gaseous Tritium Source (WGTS)
- an electron transport and tritium pumping section
- a system of two electrostatic spectrometer for energy analysis of electrons
- a semi-conductor detector

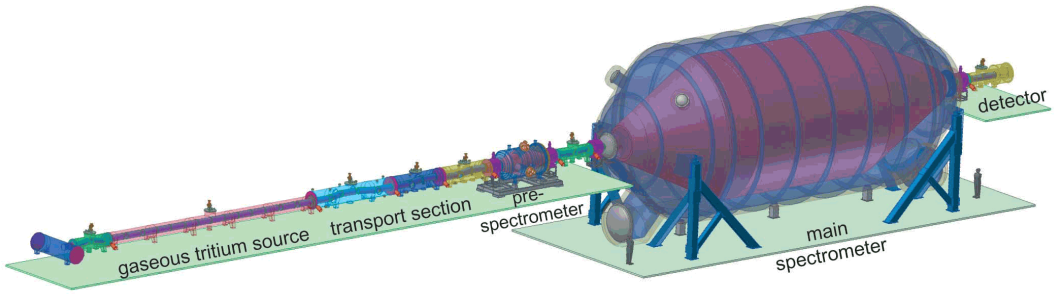

Figure 2: The 70 m long KATRIN setup with its major components: a) the windowless gaseous tritium source WGTS, b) the transport elements, consisting of an active pumping part and a passive cryotrapping section, c) the two electrostatic spectrometers and d) the detector.

The high sensitivity of the KATRIN experiment will be reached by a special type of spectrometers, so-called MAC-E-Filters (Magnetic Adiabatic Collimation combined with an Electrostatic Filter). This type of spectrometer was first proposed in [4]. The use of such a spectrometer for the neutrino mass determination was described in [5, 6]. It combines high luminosity and low background with a high energy resolution, both essential for determination of the neutrino mass from the measurement of the endpoint region of a beta spectrum.

2 Monitoring of high voltage on main spectrometer

The determination of neutrino mass requires the precise knowledge of the energy of electrons in the analyzing plane of the main spectrometer. This energy is determined by the retarding electrostatic potential at the analyzing plane and the scanning potential applied to the source. The precise measurement of the scanning voltage, which will not exceed 100 V, does not represent any problem. However, the challenge is to measure the retarding voltage of about 18 kV with a 50 mV precision, because the numerical studies [7] have shown that an unrecognized shift of retarding energy by 50 meV would result in the systematic error of the mass of neutrino as large as 40 meV which is a substantial part of the expected KATRIN sensitivity to the neutrino mass.
Two methods will be simultaneously utilized for monitoring the retarding potential:

- The retarding voltage of the KATRIN main spectrometer will be reduced by a precision high-voltage divider [8] down to a voltage below 10 V which is ideally suited for high precision digital voltmeters. Both instruments, divider and voltmeter, exhibit a drift and must be regularly calibrated.

- Monitor spectrometer serving as independent monitoring device on that will be applied the same high voltage like on main spectrometer (Figure 3). For the checking of the voltage by the monitor spectrometer, the energetically well-defined and sharp monoenergetic electron sources will be used like natural standard. Using this method, the possible unrecognized drift of divider and voltmeter can be detected and corrections may be done.

  For this purpose, two kinds of electron sources with energy of electrons close to the tritium endpoint are intended:

  - the K-conversion electrons from the 32 keV transition in $^{83\mathrm{m}}\mathrm{Kr}$ (K-32) having the energy of 17824.3(2) eV [9] and natural width of 2.8 eV [10].
  - the photoelectrons ejected by 26 keV gamma-ray photons of $^{241}\mathrm{Am}$ from the atomic K-shell of cobalt foil. The energy of photoelectrons calculated as the difference of gamma ray and binding energies amounts to 18635.8(2) eV. The line width is given by the cobalt atomic K-level and amounts to 1.3 eV [1]

Actually, for the monitoring it is not very important to know precise electron energy for particular source but a high stability and reproducibility of electron energy deduced from the measured spectra is substantial.

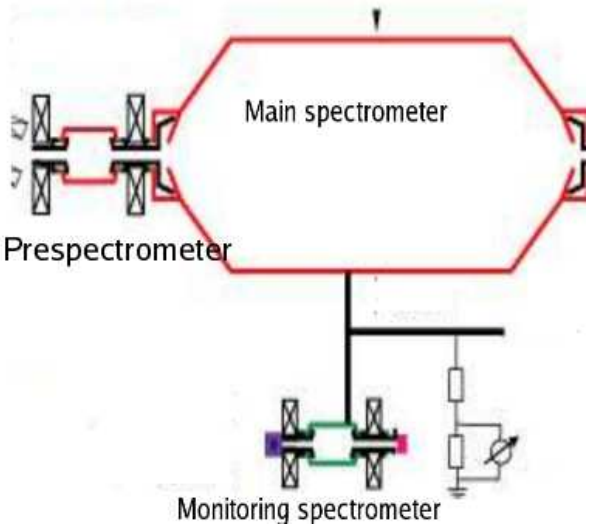

Figure 3: The setup of the monitor spectrometer and the main spectrometer.

3 Numerical simulation

Currently the vacuum evaporated solid generator type ^{83}Rb/^{83m}Kr source is developed at NPI Rez. The quality of the sources is tested in the electron spectrometer. Owing to the ambitious demand, energy stability and reproducibility at 50 meV level, very careful and detailed analysis of the measured electron spectra is necessary. For this purpose the simulation of the spectrometer output data file will be very useful. The measured value of energy of the conversion electrons depends on both the statistical uncertainty and the systematic uncertainty. The proposed simulation will be used for investigation of systematic uncertainties.

3.1 Motivation

Up to this day, the nuclear standards for electron spectroscopy do not exist, contrary to the gamma spectroscopy. Nevertheless for the KATRIN monitoring spectrometer, a radioactive source with monoenergetic electrons is needed. For this reason, we are developing a source based on $^{83\mathrm{m}}\mathrm{Kr}$. For this standard, it is needed to know the position (energy) of conversion line in spectrum precisely. The energy of conversion electron or, in other words, atomic levels in the source vary with a distribution of electrons in cloud caused by orbitting electrons and also due to chemical bonding between substrate and Rb/Kr layer. Also, with decay of rubidium into krypton, one originates electric charge and it can change distribution of charge in electron clouds and it affects atomic levels. The shape of electron spectrum, its low-energy range, also depends on energy loss due to the penetration of electrons throw matter of source. In order to investigate influences of these effects, at first we have to investigate how energy of conversion line depends on instabilities or, more accurately, uncertainties of voltage of power supply and, of course, on uncertainty of measured voltage of voltmeter.
We investigate these effects using the spectrometer ESA12[1] (Figure 4) [11] in Řež.

[1]The spectrometer ESA12 is differential spectrometer unlike all KATRIN's spectrometers which are integral spectrometers.

Figure 4: Electrostatic spectrometer ESA12 at NPI Řež.

Unfortunately we cannot apply high voltage of 17 kV on this spectrometer, i.e. the conversion line K-32 cannot be directly investigated. Thus we use conversion electrons L_1 of transition 9.4 keV in ^{83m}Kr. We suppose, if position of K-32 changes due to the above effects, the energy of L_1-9.4 line proportionally changes too.
The conversion line L_1-9.4 is for this purposes suitable because this line is very intensive. It is circa two times wider (FWHM = 5.3 eV [10]) than K-32 , however, it is unsubstantial in this case for our aims.

3.2 Physical background and philosophy of a computer code for the simulations

The electrostatic spectrometer at Řež can operate in several modes. One of them is so called retardation mode [11]. In this mode, we apply the voltage both on the analyzing electrode and on the source. During the measurement, the voltage on electrode is fixed and we change voltage on source by fixed step (0.5 eV) in order to measure electron spectrum in the required energy range. This mode is used for more delicate and accurate measurements. For this mode, we have developed the computed code which simulate the spectrometer output data file corresponding to the electron spectrum given by the input data.
The shape of the conversion line is described by Lorentzian function. However, the spectrometer, by which spectrum is taken, has got a finite resolution, so, in practise, the shape of it is described by a folding (convolution) of Lorentzian curve $L(E)$ and a apparatus function $G(E)$, i.e.

$$L(E) \star G(E) \; = \; \int\limits_{-\infty}^{\infty} L(E')G(E-E')\mathrm{d}E',$$

where for $G(E)$ stands

$$\int\limits_{-\infty}^{\infty} G(E)\mathrm{d}E = 1.$$

In our case, that means for spectrometer ESA12 at Řež, the apparatus function can be very well described by Gaussian function [11], i.e. the final term for convolution is

$$\int\limits_{-\infty}^{+\infty} A\frac{\left(\frac{\Gamma_L}{2}\right)^2}{\left(E'-E_0\right)^2+\left(\frac{\Gamma_L}{2}\right)^2}\frac{1}{\sqrt{2\pi}\sigma}\exp\left[-\frac{\left(E-E'\right)^2}{2\sigma^2}\right]\mathrm{d}E', \tag{1}$$

where A is height (or more accurately amplitude) of the peak, Γ_L is FWHM of Lorentzian function, E_0 energy of the conversion line and $\sigma = \frac{1}{2\sqrt{2\ln 2}}\Gamma_G$, where Γ_G is FWHM of Gaussian function.
Since the integral (1) contains e^{-x^2}-like function, the most appropriate is to compute this integral by Gauss-Hermite quadrature [12] (sometimes called only Hermite quadrature). The general formula for Gauss-Hermite quadrature is

$$\int\limits_{-\infty}^{+\infty} f(x)w(x) = \sum_{j=1}^{m} w_j f(x_j), \tag{2}$$

where $f(x)$ is an arbitrary function, $w(x) = \mathrm{e}^{-x^2}$ is so called weight function, x_j is j-th root of Hermite polynomial of the n-th degree and w_j weight corresponding to the root x_j. We have tried Hermite quadratures for several orders[2]. Eventually we have decided Hermite

[2]We have tried quadratures of 10th, 14th, 18th, 20th, 22nd, 26th order, and from the 20th order, the value of integral (1) is not changed.

quadrature of twentieth order, the weights and roots were computed by program Mathematica [13]. We have computed the weights from the formula

$$w_i = \frac{2^{n-1} n! \sqrt{\pi}}{n^2 [H_{n-1}(x_i)]^2},$$

where $H_n(x)$ is Hermite polynomial of n-degree.
In order to use Hermite quadrature, we have rewritten the integral (1) to "Hermite quadrature" form, where we have used the replacement $\frac{(E-E')^2}{2\sigma^2} = E_1$. Finally we have got formula

$$\int_{-\infty}^{+\infty} A \left(\frac{\Gamma_L}{2}\right)^2 \frac{1}{\left(E - 2\sigma^2 E_1 - E_0\right)^2 + \left(\frac{\Gamma_L}{2}\right)^2} \mathrm{e}^{-E_1^2} \mathrm{d}E_1. \tag{3}$$

The energy of electrons E is proportional to the retarding voltage U_S that is applied on source, for this type of the spectrometer [11]

$$E_{kin} = e \left(U_S + \frac{U_C}{0.56}\right),$$

where U_C is voltage that is applied on analyzing electrode. The numerical value 0.56 represents so called spectrometer constant that depends on the spectrometer dimensions. Measurements are performed at $\mathrm{U_C}$ = 146 which implies that electrons with kinetic energy 260 eV can go through the spectrometer analyzing electrodes and hit the detector. The energy of 260 eV amounts to the energy resolution 2.9 eV (i.e. 1.1 % of $\frac{U_C}{0.56}$).

In the next paragraph, we will describe, how we have done the numerical simulations of the conversion spectrum. This simulation imitates the control program output file of the spectrum, taken by the spectrometer. This program writes measured data in a file that contains two columns. There are the voltage that is measured by voltmeter in the first column, and number of counts in the second one. This file consists of many sweeps, where one sweep represents one throughpass of the spectrum taking on.
In the first sweep for the first point of spectrum, the energy (or voltage of power supply), for instance, is V_0. We have assumed that the voltage on power supply is a normal distributed quantity. Then, for this value, we have got a value of this voltage by a random number generator, V_1 (in general, $V_0 \neq V_1$). Now we have computed a number of counts N_0 that corresponds to a theoretical spectrum, i.e. Voight function. Since, in practise, the number of counts is a Poisson distributed quantity, we, again by random number generator, have generated the realistic (or measured) number of counts N_1 (again in general, $N_0 \neq N_1$). The N_1-value, we write to a file that looks like the output file from the real measurement.
The voltage V_1 is reduced by a precision high-voltage divider down to a voltage below 20 V, this reduced voltage V_1' is measured by a voltmeter. Once again we have assumed that a voltage on the voltmeter is a normal distributed quantity, and therefore, by random number generator, we have got the realistic measured voltage V_1''. We write the voltage V_1'' to the file and this one corresponds to number of counts N_1. Then we go ahead to the next point where we repeat the same procedure as in previous point. When we have finished the first sweep, in analogy with a scan procedure of the spectrometer, we jump to the beginning of the

measured spectrum, and we get in the next or another sweep for the voltage V_0 the voltage V_2 (once again in general $V_0 \neq V_1 \neq V_2$), for the number of counts N_0, we get number of counts N_2 ($N_0 \neq N_1 \neq N_2$ in general), and the same we do with voltage on the voltmeter.
Typically we have simulated one thousand of sweeps. From this sweeps, we reconstructed the electron spectrum. We have counted up the number of counts of each sweep that belong to the certain bin (for example $\left(E - \frac{\Delta}{2}, E + \frac{\Delta}{2}\right\rangle$), where Δ is the sorting (or binning) step). The resultant number of counts, we re-count per a unit of time. In our case this is one second, because we have assumed that the spectrometer have spent one second when it has taken the data in one point of spectrum.

3.3 Results

The simulated data have been fitted by ROOT [14] and using the MINUIT package with Migrad minimization method. We have used two parametrization of the Voight function for this fit. Since we are interesting only in the determination of the position of the conversion line, in the first parametrization, we have assumed that the Voight function is folded from the Lorentzian and Gaussian function with the same FWHM. In the second one, we have used the parametrization where these FWHM's are different.
Thus the first parametrization has got the form:

$$V(\Gamma, A, E_0) = L(\Gamma, E_0, A) \star G(\Gamma),$$

where $V()$ is Voight function, Γ's are the FWHM's of Lorentzian $L()$ and Gaussian function $G()$, E_0 is the energy of the conversion electrons, and A is a height of the peak. Since this convolution has not got again an analytical solution, we should compute and subsequently fit in the numerical form. We have used once again the Gauss–Hermite quadrature of the 20th order. Therefore we have written the Voight function (in according to (2))in the form:

$$A \sum_{j=0}^{20} \left\{ \left[\frac{1}{\frac{2(E-E_0)}{\Gamma} - H_{20}(x_j)} \right]^2 + 1 \right\} w_j, \tag{4}$$

where A is the height of peak, E_0 the energy of conversion electrons, $H_{20}(x_j)$ is the value of Hermite polynomial of 20th order for x_j-root of this one, and w_j is the weight corresponds to x_j-root. This integral has been computed again by Gauss-Hermite integration. In this case, we have once again used the Gauss-Hermite quadrature of the 20th order. The results of this fit are plotted in the Figure 5.
The second parametrization has got the different FWHM's, i.e. Lorentzian Γ_L and Gaussian Γ_G.

$$V(\Gamma_L, \Gamma_G, A, E_0) = L(\Gamma_L, E_0, A) \star G(\Gamma_G),$$

In order to fit the Voight function numerically, we have overwritten this one in the form:

$$\frac{A}{4\sqrt{\pi}} \sum_{j=0}^{20} \left\{ \left[\frac{1}{\frac{\left(E - \sqrt{2}\Gamma_G \; H_{20}(x_j) - E_0\right)}{\Gamma_L}} \right]^2 + \frac{1}{4} \right\} w_j,$$

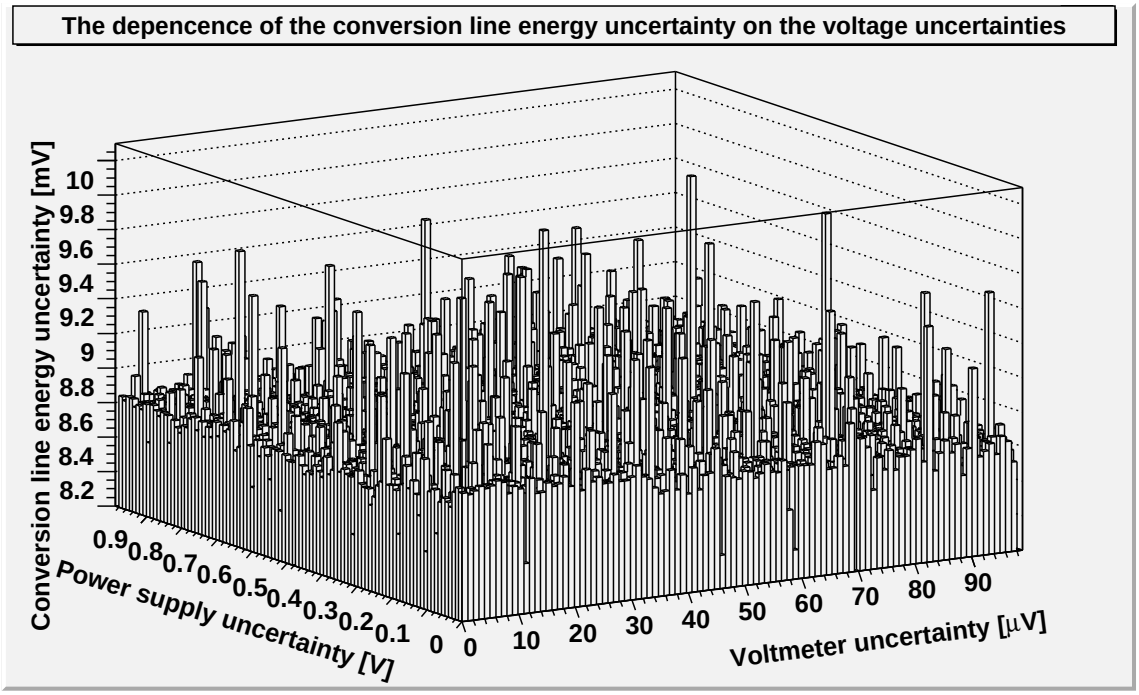

Figure 5: The dependence of the conversion line energy uncertainty on the voltage uncertainties for the parametrization with the same FWHM's for Lorentzian and Gaussian function.

the variables have the same meaning as in (4). How we can see from the Figure 6, this parametrization is more precise than the previous one.
Now we will discuse if both parametrizations give the close values of the line energy uncertainty. Therefore we compare both parametrization (we have subtracted the first from the second one). This is plotted in the Figure 7. From this figure, we can see that both parametrization are equivalent because most of the differences is equal or very close to zero. The region of the plotted data was chosen by reason of the voltmeters which are used in Řež have got the voltage uncertainty (2 μV for Fluke, and 40 μV for Solartron), and of the Řež's power supply (its voltage uncertainty is 0.4 V).
Now we focus to results of the first parametrization. When we look at the Figure 5, we can see that, in our investigated range, all data are concentrated around the plane with vertical coordinate equal to 8.8 mV. We look more closely in this data. We do several cuts of this plane, firstly in power supply direction, i.e. we fix voltmeter voltage uncertainty, and then in voltmeter direction, i.e. we fix power supply uncertainty.
At first, we fixed the voltage uncertainty and we will investigate how does the line energy uncertainty depend on the power supply uncertainty. We have fixed following voltmeter uncertainties, 2 μV (Fluke voltmeter - Figure 8), 40 μV (Solartron voltmeter - Figure 9), and 80 μV (Figure 10).
These ones have been fitted again by constant line. The line energy uncertainty is very close to 8.80 mV.
And then we have fixed the power supply uncertainty (once again the same values as in previous case). For the line energy uncertainty, we have got almost 8.80 mV from the fit of these histograms (pictured in the Figure 11, 12, and 13).

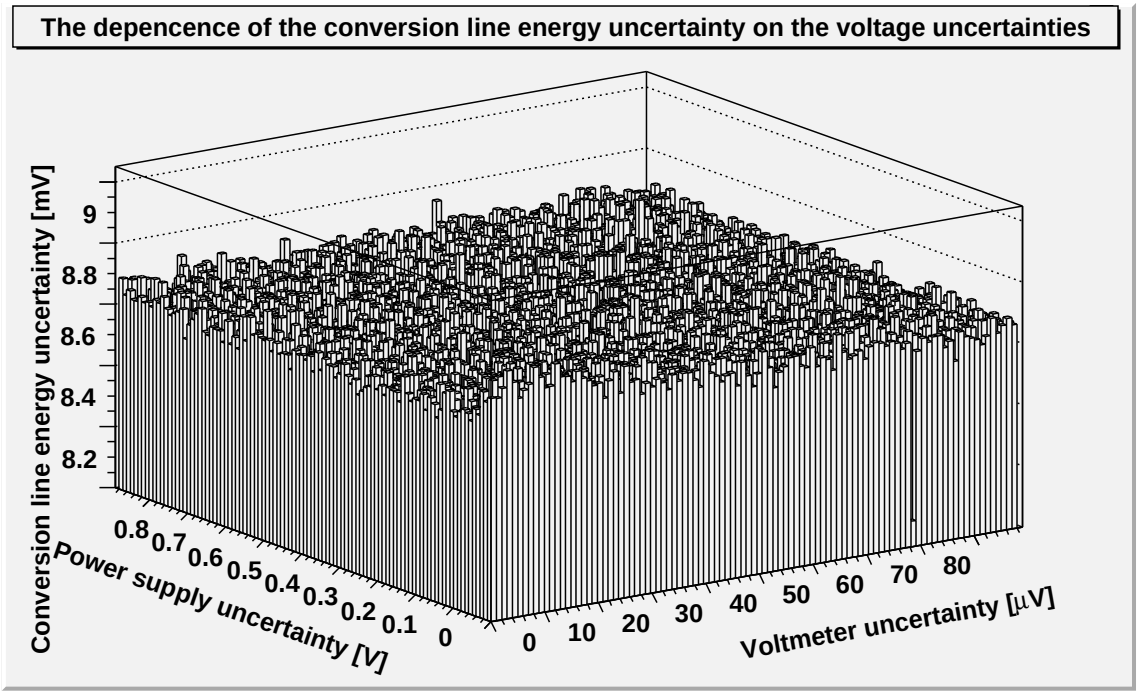

Figure 6: The dependence of the conversion line energy uncertainty on the voltage uncertainties for the parametrization with the different FWHM's for Lorentzian and Gaussian function.

Now we will be interested in the parametrization with the different FWHM's both in Gaussian function and Lorentzian function. We again fixed the voltmeter uncertainties, the same as in previous case. The relevant histograms are pictured in the Figures 14, 15, and 16 .
How we can see in previous histograms, the data are very close to constant line in this region and then we tried to fit them by constant line. The uncertainty of line energy determination is, in all cases, very close to 8.84 mV.
Now we fix the power supply uncertainties. We have done the same procedure as in previous case. We have chosen the following power supply uncertainties: 0.1 V (Figure 17), 0.4 V (Figure 18), and 0.8 V (Figure 19).
When we fitted these histogram by constant line, we have got the line energy uncertainty, once again, very close to 8.84 mV.

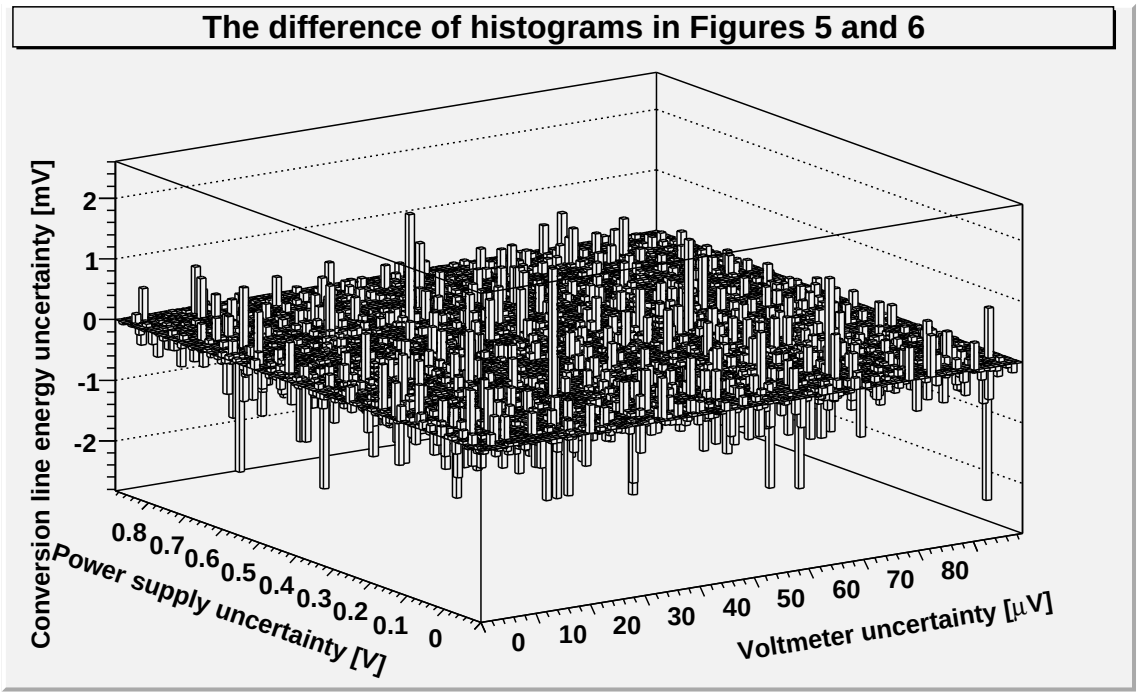

Figure 7: This plot shows that the differences between both parametrization are very close to zero, in other words the both parametrization are equivalent.

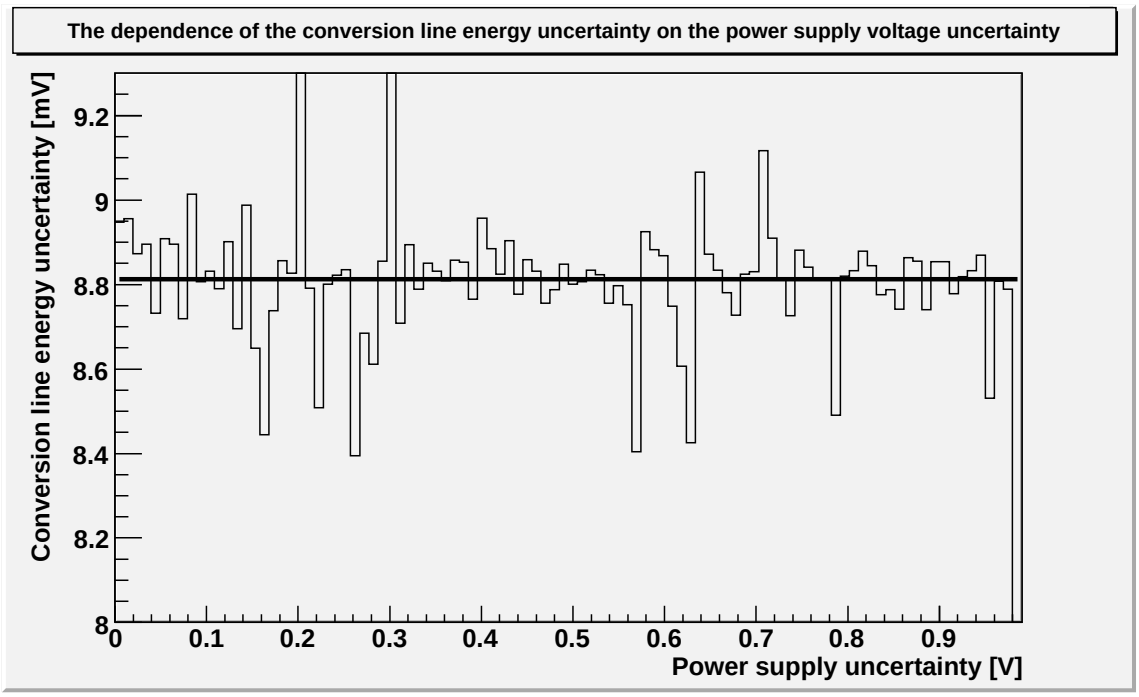

Figure 8: The dependence of the conversion line energy uncertainty on the power supply voltage uncertainties for fixed voltmeter uncertainty equal to 2 μV.

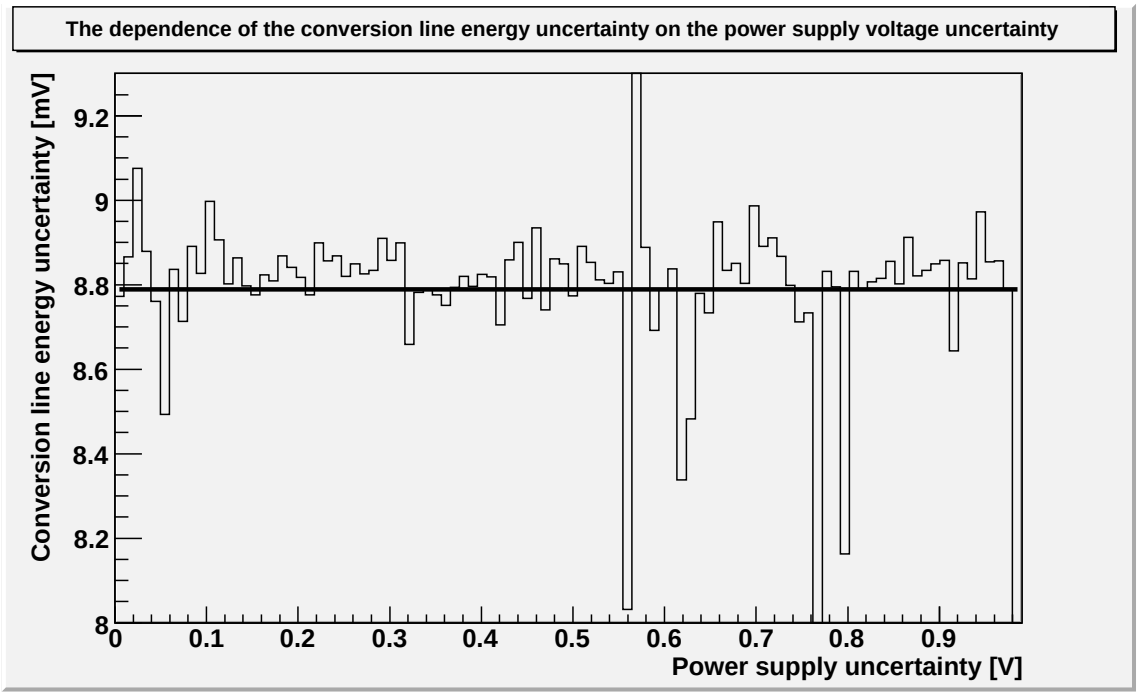

Figure 9: The dependence of the conversion line energy uncertainty on the power supply voltage uncertainties for fixed voltmeter uncertainty equal to 40 μV.

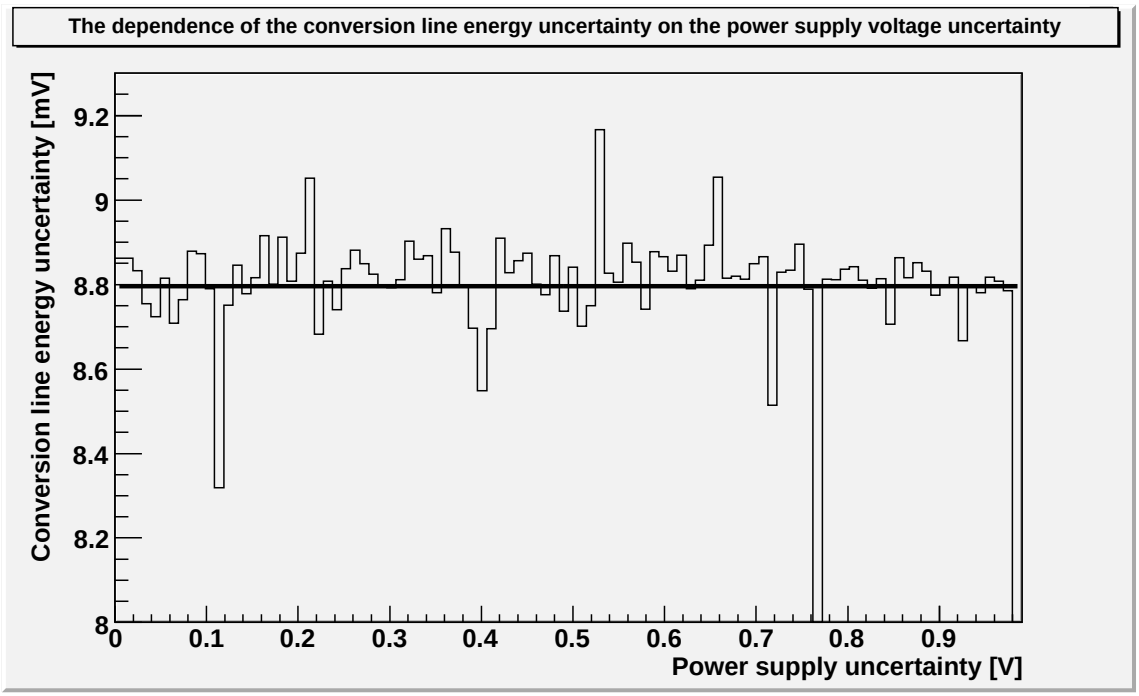

Figure 10: The dependence of the conversion line energy uncertainty on the power supply voltage uncertainties for fixed voltmeter uncertainty equal to 80 μV.

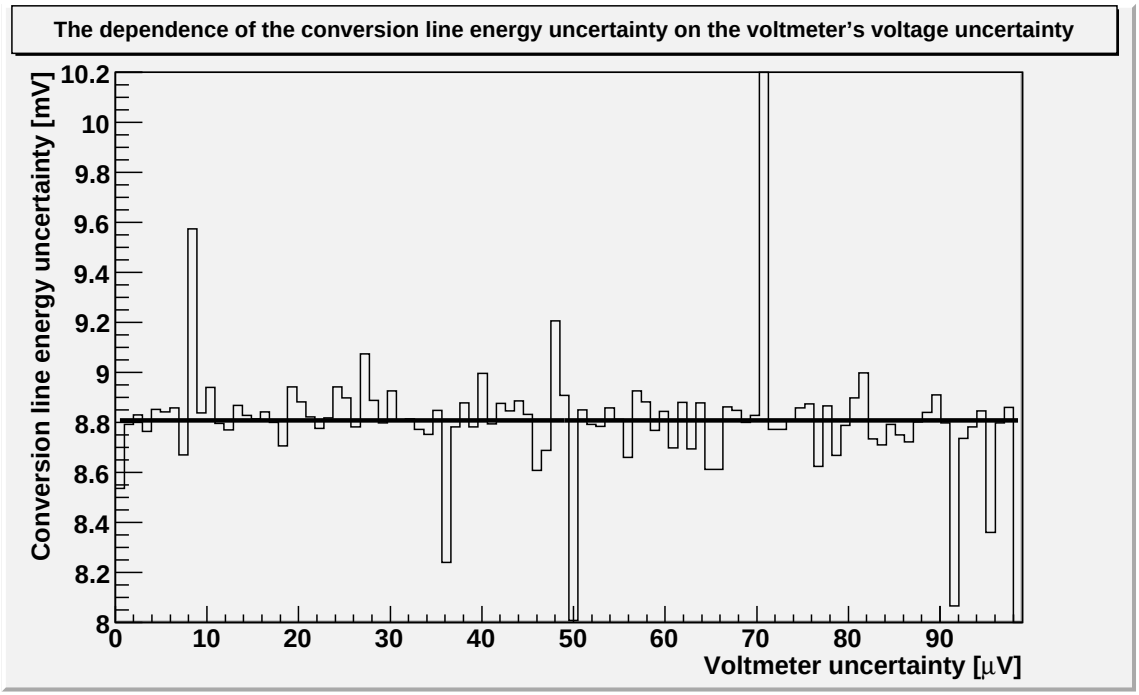

Figure 11: The dependence of the conversion line energy uncertainty on the voltmeter voltage uncertainties for fixed power supply uncertainty equal to 0.1 V.

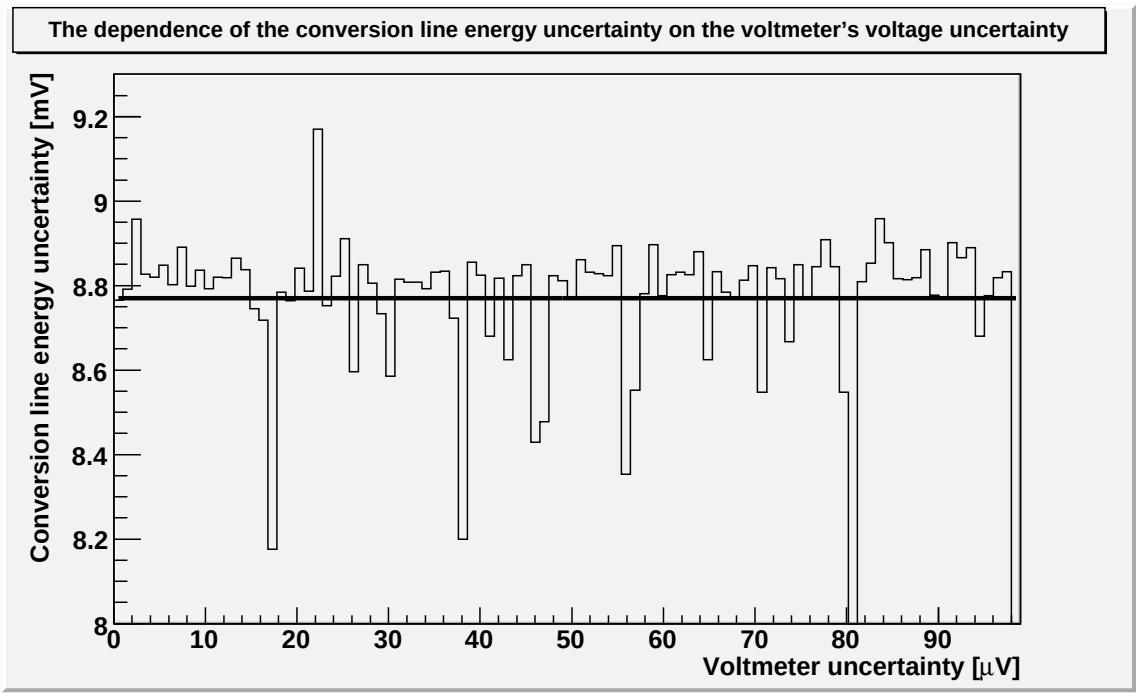

Figure 12: The dependence of the conversion line energy uncertainty on the voltmeter voltage uncertainties for fixed power supply uncertainty equal to 0.4 V.

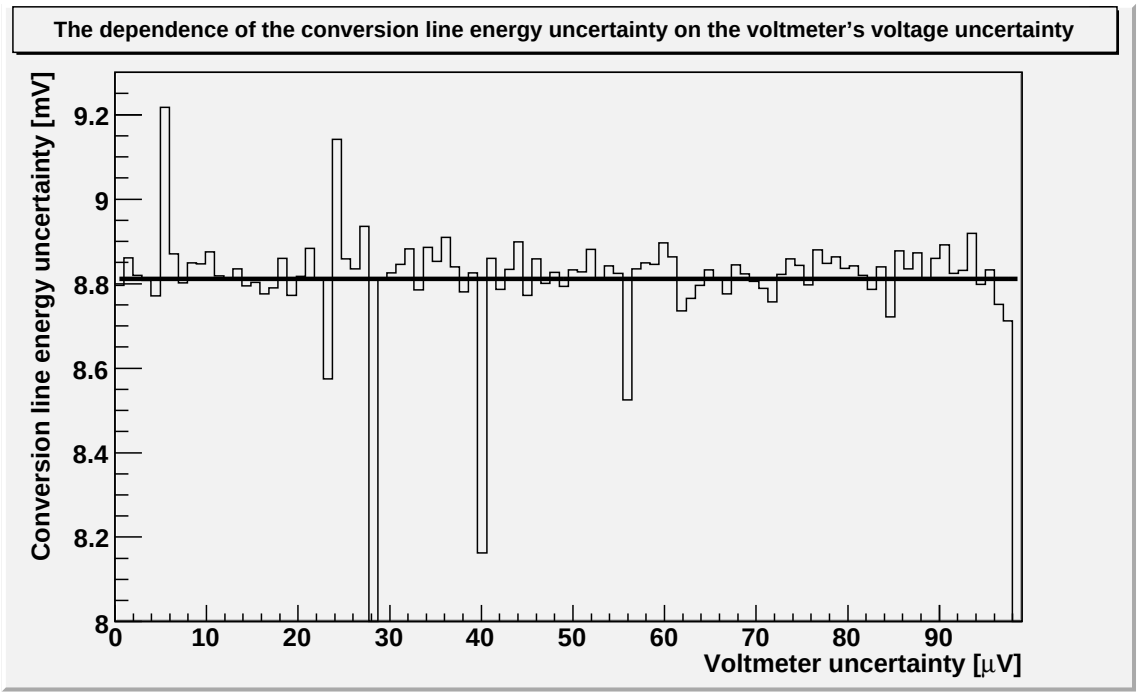

Figure 13: The dependence of the conversion line energy uncertainty on the voltmeter voltage uncertainties for fixed power supply uncertainty equal to 0.8 V.

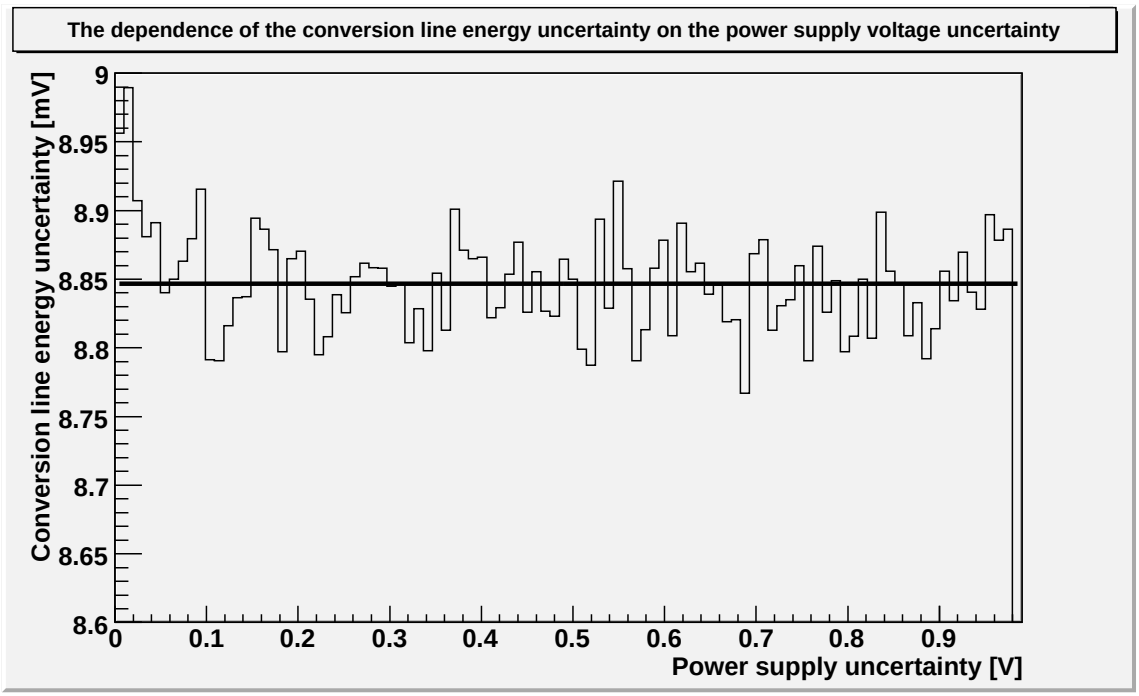

Figure 14: The dependence of the conversion line energy uncertainty on the power supply voltage uncertainties for fixed voltmeter uncertainty equal to 2 μV.

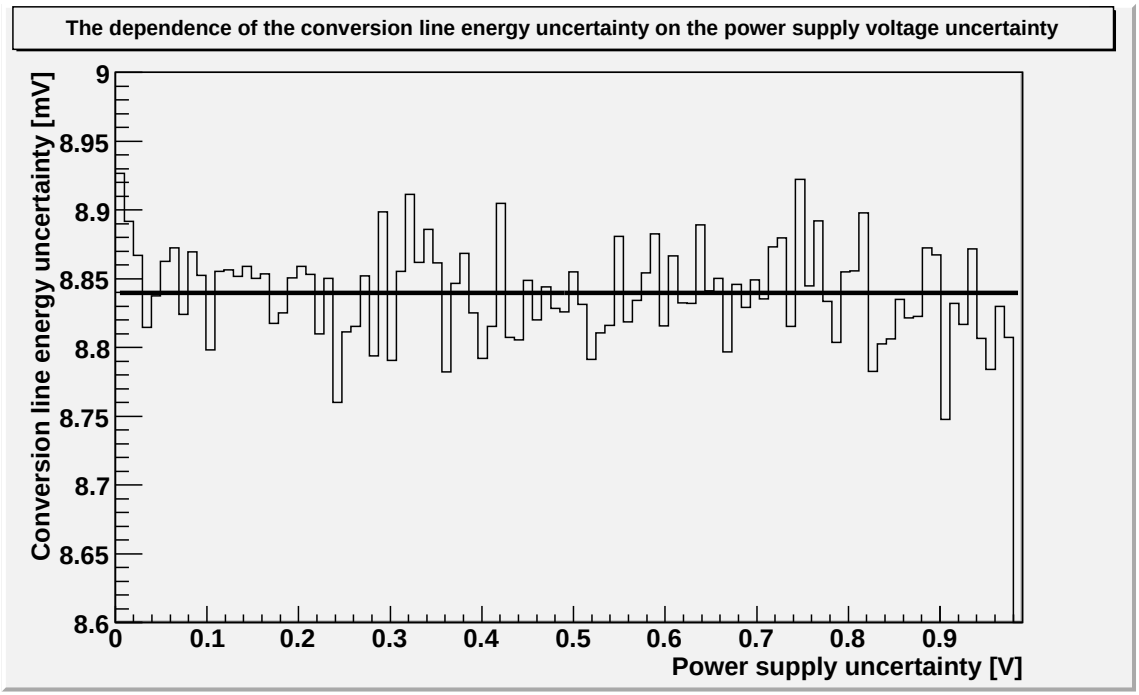

Figure 15: The dependence of the conversion line energy uncertainty on the power supply voltage uncertainties for fixed voltmeter uncertainty equal to 40 μV.

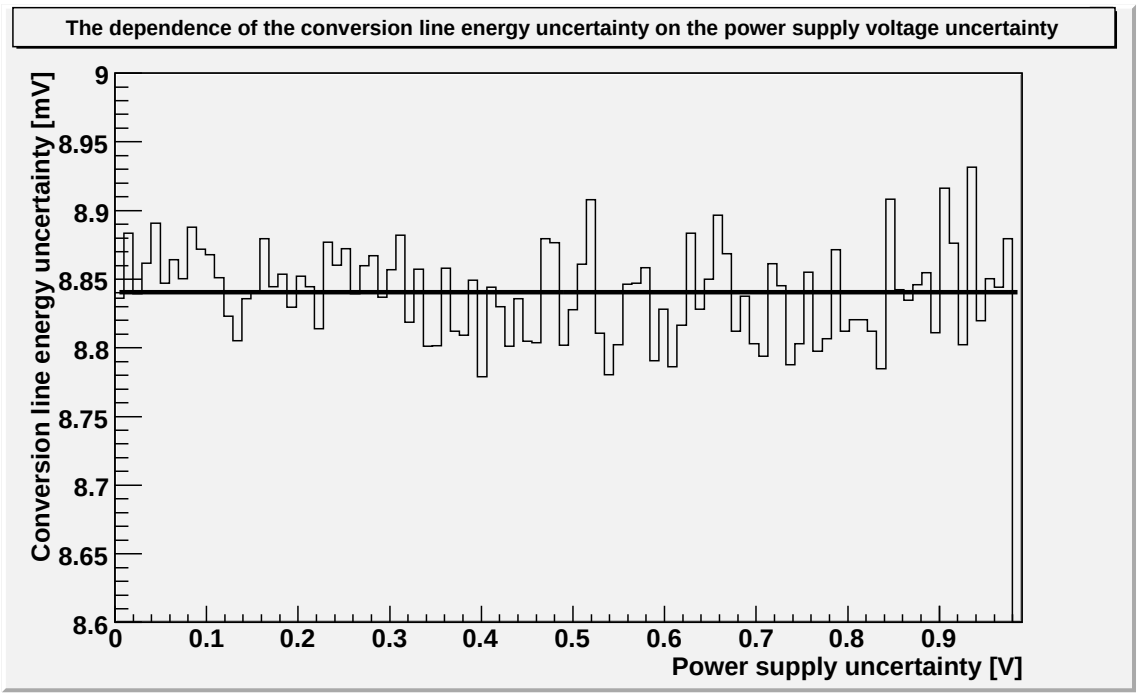

Figure 16: The dependence of the conversion line energy uncertainty on the power supply voltage uncertainties for fixed voltmeter uncertainty equal to 80 μV.

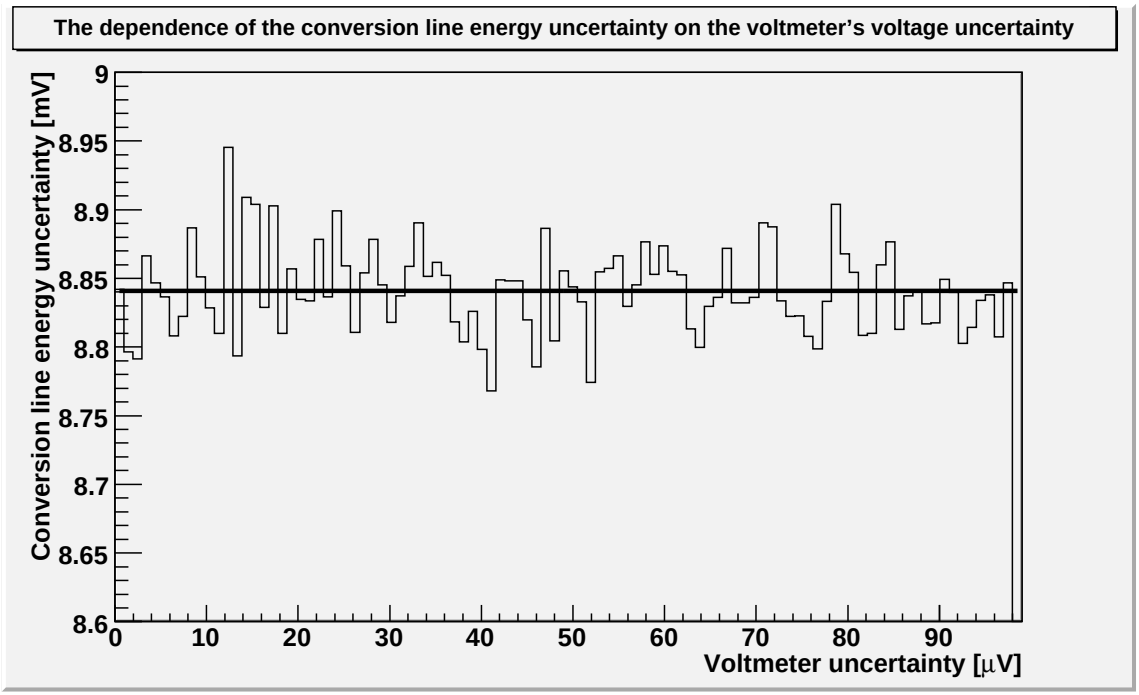

Figure 17: The dependence of the conversion line energy uncertainty on the voltmeter voltage uncertainties for fixed power supply uncertainty equal to 0.1 V.

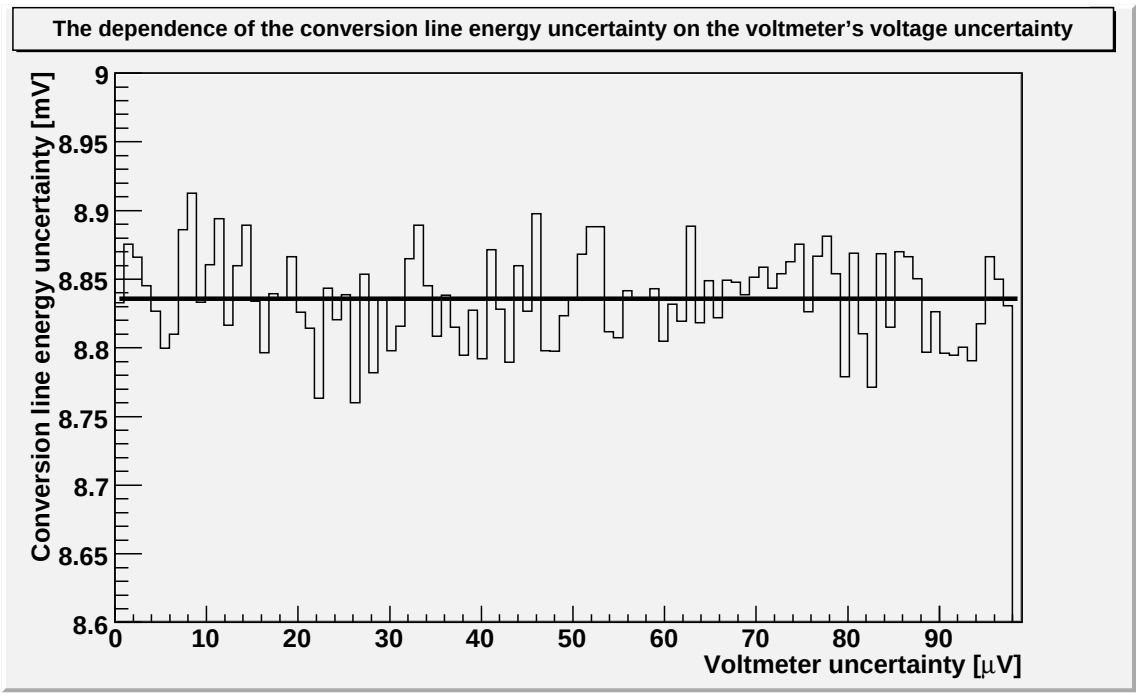

Figure 18: The dependence of the conversion line energy uncertainty on the voltmeter voltage uncertainties for fixed power supply uncertainty equal to 0.4 V.

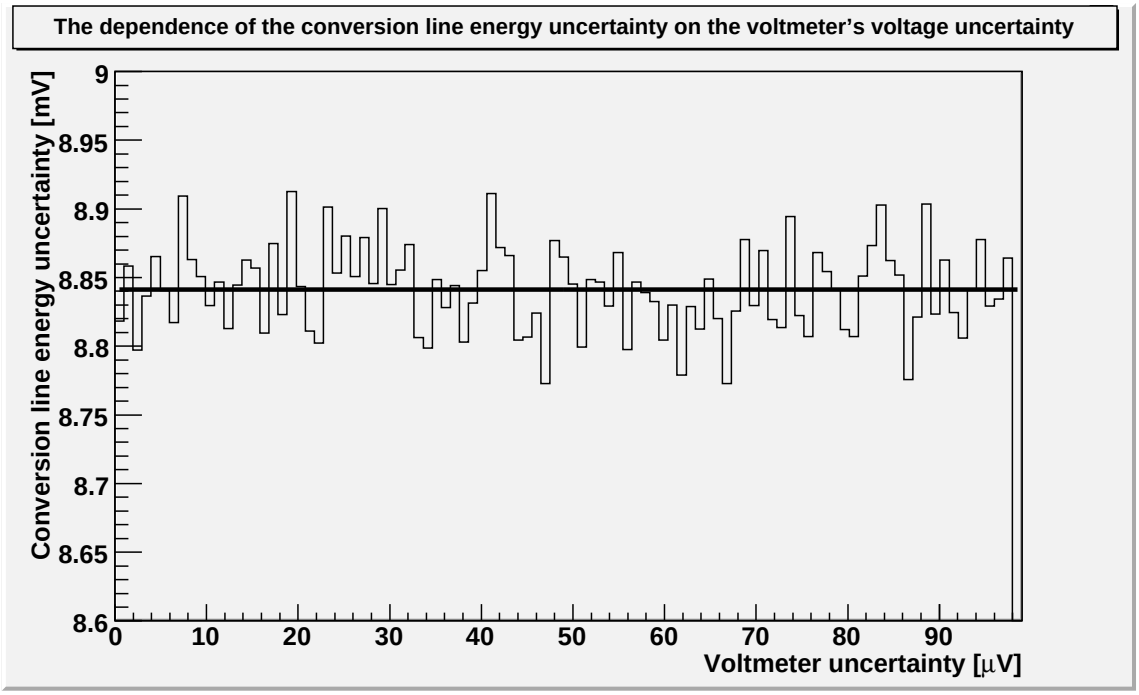

Figure 19: The dependence of the conversion line energy uncertainty on the voltmeter voltage uncertainties for fixed power supply uncertainty equal to 0.8 V.

4 Summary and conclusion

In this work, we have concentrated ourselves on the influence of the uncertainties of the voltage of the power supply and voltmeter on the line energy uncertainty. This is one of the first steps in the procedure of preparing a nuclear standard for the electron spectroscopy. We find that in the range of voltage uncertainties that is in our focus the uncertainty of line energy is around 8.8 mV. This value is sufficient for further Řež's measurement with the electron spectrometer. Since the line energy uncertainty also depends on the strength of the radioactive source (on the height of the peak) through the uncertainty of the number of counts (its square root) that occur in minimize procedure, so for a stronger source, the line energy uncertainty will be than smaller.

Appendix

Software

In our computer simulation, we have used several software frameworks. The own program for the simulation of the electron conversion spectrum was written in program language C. In program code, we used the roots of Hermite polynomial; to acquire the root values we have used the famous program framework for symbolic computing - Mathematica. The final part of numerical simulation - the fitting of data and plotting of the histograms - was created in ROOT.

ROOT is an object oriented framework aimed at solving the data analysis of high energy physics. It was developed in the context of the NA49 experiment at CERN. NA49 has generated an impressive amount of data, around 10 Terabytes per run. This rate provided the ideal environment to develop and test the next generation data analysis. ROOT contains CINT interpreter (C++ interpreter) that serves to a communication with a user.

Minuit is projected as a tool to find the minimum value of a multi parameter function and analyze the shape of the function around its minimum. The principal application is statistical analysis, working on chi-square or log-likelihood function, to compute the best fitted parameter values and their uncertainties, including correlations between the parameters. Minuit was, in origin, written in FORTRAN, and consecutively it has been converted to C++. Later it was integrated to ROOT as its package.
One of the minimization method in Minuit, that we used, is called MIGRAD. This is the best minimizer for almost all function. The minimizing technique currently implemented in MIGRAD is a stable variation of the Davidon-Fletcher-Powell variable-metric algorithm [15]. This algorithm converges to the correct error matrix as it converges to the function minimum.

References

[1] KATRIN collaboration, KATRIN Design Report 2004, Report FZKA 7090, NPI Řež EXP-01/2005, MS-KP-0501.

[2] Ch. Kraus et al., Eur. Phys. J. C40 (2005) 447

[3] V.M. Lobashev et al., Nucl. Phys. B91 (2001) 280

[4] G. Beamson et al. , J. Phys. Sci. Instrum. 13 (1980) 64

[5] V.M. Lobashev, Nucl. Inst. and Meth. A240 (1985) 305

[6] A. Picard et al., Nucl. Inst. Meth. B63 (1992) 345

[7] J. Kašpar et al., Nucl. Instr. and Meth. A527 (2004) 423

[8] R. Marx, IEEE Trans. Instr. Meas. Vol. 50, No. 2 (2001) 426

[9] D. Vénos et al., Nucl. Inst. and Meth. A560 (2006) 352

[10] A. Picard et al., Z. Phys. A342 (1992) 71

[11] D. Varga et al., Nucl. Inst. and Meth. 192 (1982) 277

[12] E. W. Weisstein, "Hermite-Gauss Quadrature." From MathWorld–A Wolfram Web Resource. http://mathworld.wolfram.com/Hermite-GaussQuadrature.html

[13] http://www.wolfram.com/

[14] http://root.cern.ch/

[15] W. C. Davidon, Variable metric method for minimization, SIAM Journal on Optimization 1 (1991) 1